

Inelastic co-tunneling through an excited state of a quantum dot

M. R. Wegewijs, Yu. V. Nazarov

*Department of Applied Physics, Faculty of Applied Science,
Delft University of Technology, Lorentzweg 1, 2628 CJ Delft, The Netherlands*

We consider the transport spectroscopy of a quantum dot with an even number of electrons at finite bias voltage within the Coulomb blockade diamond. We calculate the tunneling current due to the elastic and inelastic co-tunneling processes associated with the spin-singlet ground state and the spin-triplet first excited state. We find a step in the differential conductance at a bias voltage equal to the excitation energy with a peak at the step edge. This may explain the recently observed sharp features in finite bias spectroscopy of semi-conductor quantum dots and carbon nanotubes. Two limiting cases are considered: (i) for a low excitation energy, the excited state can decay only by inelastic co-tunneling due to Coulomb blockade (ii) for a higher excitation energy the excited state can decay by sequential tunneling. We consider two spin-degenerate orbitals that are active in the transport. The nonequilibrium state of the dot is described using master equations taking spin degrees of freedom into account. The transition rates are calculated up to second order in perturbation theory. To calculate the current we derive a closed set of master equations for the spin-averaged occupations of the transport states.

I. INTRODUCTION

Transport spectroscopy provides information on the excited states of quantum dots.¹ Outside the Coulomb blockaded regions (“diamonds”), peaks in the differential conductance can be observed, which linearly shift with the gate voltage.² Such a peak indicates that an excited state has entered the transport voltage window. Recently, De Franceschi et al. observed new features in the spectroscopy data of a vertical semiconductor quantum dot coupled relatively strong to the leads.³ *Inside* several Coulomb diamonds with an even number of electrons they observed a step in the differential conductance with a peak at the step edge for a quantum dot with six electrons. In contrast to the peaks outside the diamond, this feature depends very weakly on the gate-voltage. This was interpreted as being due to *inelastic co-tunneling* through an excited state of the dot. It was pointed out that the sharpness of the step is determined either the temperature or by the broadening of the excited level, both of which are small energy scales compared to the widths of the first-order tunneling peaks. This provides an new spectroscopic tool for studying excited levels in quantum dots. Similar features were observed in the transport spectroscopy of carbon nanotubes obtained by Nygård et. al.⁴ Here also, the gate voltage independent features at finite bias voltage were clearly seen in consecutive Coulomb diamonds with an even number of electrons. The observed peaks at the step edges were attributed to Kondo-physics. In both experiments a Kondo effect was observed at zero bias voltage in a magnetic field. The occurrence of Kondo peaks in the differential conductance, although of different origin, indicates a relatively strong coupling to the leads.⁵⁻⁷

Motivated by these experiments, we have calculated the co-tunneling current through an excited level of a quantum dot using a master equation approach. We investigate the possibility that the observed features arise from changes in the nonequilibrium occupations of the states in the dot. Such changes are caused by voltage-dependence of co-tunneling processes. We find that a peak structure in the differential conductance can develop at the onset of inelastic co-tunneling. We consider the possible regimes defined by the energy of the excited level relative to the addition energy. Two possible cases are distinguished:³ (i) for low excitation energy, the excited state can decay only by inelastic co-tunneling due to Coulomb blockade; (ii) for higher excitation energy the excited state can decay by sequential tunneling. We take the spin degrees of freedom into account and derive master equations for the nonequilibrium occupations of the relevant states, which are averaged over the spin projections. The case (i) has recently been considered by M. Eto⁸ without taking the spin degrees of freedom into account.

The plan of the chapter is as follows. In Sec. II we introduce a model for the transport spectroscopy of a quantum dot. The low bias elastic co-tunneling current is discussed in Sec. III and in Sec. IV we consider the different regions of the Coulomb diamond at higher bias where inelastic co-tunneling dominates the transport. Our conclusions are presented in Sec. V.

II. TRANSPORT SPECTROSCOPY

We consider a quantum dot connected to two leads L and R and one gate electrode G . The dot is modeled by the Hamiltonian $H = H_{\text{sp}} + H_{\text{el}} + H_{\text{ex}}$. The discrete single particle states are labeled by $d = 1, 2, \dots$ and are spin degenerate, $s = \uparrow, \downarrow$:

$$H_{\text{sp}} = \sum_{ds} \varepsilon_d n_{ds},$$

where $n_{ds} = a_{ds}^\dagger a_{ds}$ is the number operator of level ds . We describe the electron-electron interactions in the classical electron liquid picture (Coulomb blockade model)¹. The electrostatic energy depends on the total number of electrons $N = \sum_{ds} n_{ds}$ in the dot and on the voltages on the electrodes, which couple to the island through the capacitances C_L, C_R, C_G (total capacitance $C = \sum_{k=L,R,G} C_k$):

$$H_{\text{el}} = \frac{1}{2} N (N - 1) U + \left(\frac{1}{2} U - \sum_{k=L,R,G} \frac{C_k}{C} V_k \right) N.$$

Here $U = 1/C$ is the charging energy (we use units $e = k = \hbar = 1$). We also include an exchange term that lowers the energy of states with parallel spins:

$$H_{\text{ex}} = -J \sum_{dd's} n_{ds} n_{d's}$$

The leads are modeled as noninteracting quasi-particle reservoirs with spin degenerate states. For the left lead with states l we write $H_L = \sum_{ls} \varepsilon_l n_{ls}$ where $n_{ls} = a_{ls}^\dagger a_{ls}$ and H_R is defined similarly for the right lead (states labeled by r). The leads are assumed to be in equilibrium at chemical potential $\mu_L = \mu_R + V$ and μ_R , respectively. They are coupled to the dot by tunnel junctions. The tunneling Hamiltonian of the left junction is

$$H_{TL} = \sum_{ds} \left(H_{TLd}^\dagger + H_{TLd} \right), \quad H_{TLd} = \sum_{ls} t_{ld} a_{ls}^\dagger a_{ds},$$

and H_{TR} is defined similarly for the right junction ($L, l \rightarrow R, r$). The temperature T is assumed to be small: $T \ll \Gamma, V, \delta$, where Γ is the typical broadening of an energy level in the dot due to the coupling to the leads and δ is the relevant level spacing introduced below.

We consider here the case where the number of electrons on the dot N is *even* at zero bias voltage. Let us first consider the conditions for *sequential tunneling* transport through the dot. For transitions between the N and $N \pm 1$ electron ground states only two orbitals need to be considered. Let $|0\rangle$ denote the $N - 2$ electron ground state and d and d' label the $N/2^{\text{th}}$ and $N/2 + 1^{\text{st}}$ orbital with level spacing $\delta = \varepsilon_{N/2+1} - \varepsilon_{N/2}$. The singlet ground state then reads $|N_{0,0}\rangle = a_{d\uparrow}^\dagger a_{d\downarrow}^\dagger |0\rangle$. Here the subscripts in $|N_{S,S_z}\rangle$ indicate the spin S on the dot and its projection S_z in some arbitrary z -direction. The doublet ground states with $N \pm 1$ electrons are denoted by

$$|(N-1)_{1/2,+1/2}\rangle = a_{d\uparrow}^\dagger |0\rangle, \quad |(N+1)_{1/2,+1/2}\rangle = a_{d'\uparrow}^\dagger a_{d\uparrow}^\dagger a_{d\downarrow}^\dagger |0\rangle, \quad (1a)$$

$$|(N-1)_{1/2,-1/2}\rangle = a_{d\downarrow}^\dagger |0\rangle, \quad |(N+1)_{1/2,-1/2}\rangle = a_{d'\downarrow}^\dagger a_{d\uparrow}^\dagger a_{d\downarrow}^\dagger |0\rangle, \quad (1b)$$

The differences between the ground state energies E_N are

$$E_{NN-1} \equiv E_N - E_{N-1} = \varepsilon_{N/2} + \left(N - \frac{1}{2} \right) U - \sum_{k=L,R,G} \frac{C_k}{C} V_k,$$

$$E_{N+1N} \equiv E_{N+1} - E_N = \varepsilon_{N/2+1} + \left(N + \frac{1}{2} \right) U - \sum_{k=L,R,G} \frac{C_k}{C} V_k.$$

In order to have sequential tunneling transport it must be possible to inject an electron from the left lead and emit one to the right lead in a subsequent event:

$$\mu_L \geq E_{NN-1} \geq \mu_R \quad (3a)$$

$$\mu_L \geq E_{N+1N} \geq \mu_R \quad (3b)$$

These transport conditions translate into a stability region in the plane of bias and gate voltages, which is shown in Fig. 1. Let us express the addition energies as a function of the position (V, V_G) in this diagram. In the limit of zero bias voltage (i.e. $V = 0$ in Fig. 1), sequential tunneling transport is possible only at two isolated points: $V_G = V_G^{NN-1}$ [Eq. (3a) is satisfied] and $V_G = V_G^{N+1N}$ [Eq. (3b) is satisfied]. At these degeneracy points the number of electrons on the dot can change by one. At the intermediate gate voltages $V_G^{NN-1} < V_G < V_G^{N+1N}$ the number of electrons on the dot is stable and equal to N . Sweeping the gate voltage one thus observes the Coulomb blockade oscillations with peak spacing

$$V_G^{N+1N} - V_G^{NN-1} = (C/C_G)(\delta + U).$$

This involves the level spacing δ because the number of electrons on the dot is even. For a finite, fixed bias voltage each of these degeneracy points develops into a gate-voltage transport window, cf. Fig. 1. Equivalently, the transport conditions (3a) and (3b) require that the bias voltage exceeds a gate-voltage dependent threshold to allow the number of electrons on the dot to fluctuate. The threshold lines are (depicted in Fig. 1)

$$V_L^{NN-1} \equiv -\frac{C_G}{C - C_L} (V_G - V_G^{NN-1}), \quad (4a)$$

$$V_R^{NN-1} \equiv +\frac{C_G}{C_L} (V_G - V_G^{NN-1}), \quad (4b)$$

$$V_L^{N+1N} \equiv +\frac{C_G}{C - C_L} (V_G^{N+1N} - V_G), \quad (4c)$$

$$V_R^{N+1N} \equiv -\frac{C_G}{C_L} (V_G^{N+1N} - V_G). \quad (4d)$$

The region where the N electron ground state is stable, the N th *Coulomb diamond*, is thus delimited by $V_L^{NN-1}(V_G), V_R^{N+1N}(V_G) < V < V_R^{NN-1}(V_G), V_L^{N+1N}(V_G)$ for gate voltages $V_G^{NN-1} < V_G < V_G^{N+1N}$. The maximal bias voltage that can be applied without lifting the Coulomb blockade is

$$V_{\max}^N = \frac{C_G}{C} (V_G^{N+1N} - V_G^{NN-1}) = \delta + U. \quad (5)$$

This is achieved at the intersection of the threshold lines (4b) and (4c) (the top of the diamond) at gate voltage $V_{G \max}^N = V_G^{NN-1} + (C_L/C) V_G^{N+1N} - V_G^{NN-1}$. Similarly, $V = -V_{\max}^N$ at the intersection of lines (4a) and (4d) at $V_G = V_G^{N+1N} - (C_L/C) (V_G^{N+1N} - V_G^{NN-1})$. The addition energies relative to the electro-chemical potentials can now be expressed in terms of distance of the bias voltage to the (gate-voltage dependent) thresholds value

$$E_{NN-1} = \mu_R - \frac{C_L}{C} (V_R^{NN-1}(V_G) - V) < \mu_R, \quad (6a)$$

$$E_{N+1N} = \mu_L + \left(1 - \frac{C_L}{C}\right) (V_L^{N+1N}(V_G) - V) > \mu_L. \quad (6b)$$

Let us now consider the transport conditions for the N electron *excited* state. We assume that the lowest lying excited state is a spin *triplet*⁵,

$$\begin{aligned} |N'_{1,+1}\rangle &= a_{d'\uparrow}^\dagger a_{d\uparrow}^\dagger |0\rangle, \\ |N'_{1,0}\rangle &= \frac{1}{\sqrt{2}} (a_{d'\uparrow}^\dagger a_{d\downarrow}^\dagger + a_{d'\downarrow}^\dagger a_{d\uparrow}^\dagger) |0\rangle, \\ |N'_{1,-1}\rangle &= a_{d'\downarrow}^\dagger a_{d\downarrow}^\dagger |0\rangle. \end{aligned}$$

with energy $E_{N'} = \Delta + E_N$. The prime indicates the excited state and the excitation energy $\Delta = \delta - J$ is just the spacing between the two active levels d and d' reduced by the exchange energy. We concentrate on the change in the current due to this excited state. The effect of excited states with higher energy (such as the spin singlet at $E_N + \delta$) is disregarded. In order to have transport by sequential tunneling, the transitions between the $N+1$ and $N-1$ electron ground states and the N electron excited state must be possible:

$$\mu_L \geq E_{N'N-1} \geq \mu_R, \quad (7a)$$

$$\mu_L \geq E_{N+1N'} \geq \mu_R. \quad (7b)$$

where

$$E_{N'N-1} = E_{NN-1} + \Delta, \quad E_{N+1N'} = E_{N+1N} - \Delta \quad (8)$$

The regions in the stability diagram where the conditions (7a) and (3b) are satisfied, are delimited by another four thresholds lines for the bias voltage:

$$V_{\alpha}^{N'N-1}(V_G) = V_{\alpha}^{NN-1} \left(V_G + \frac{C}{C_G} \Delta \right), \quad (9a)$$

$$V_{\alpha}^{N'N+1}(V_G) = V_{\alpha}^{NN+1} \left(V_G - \frac{C}{C_G} \Delta \right), \quad (9b)$$

respectively, where $\alpha = L, R$. These are simply the regions in Fig. 1 where (7a) and (3b) are satisfied, shifted in gate voltage by $(C/C_G) \Delta$ towards the center of the Coulomb diamond. Outside the Coulomb diamond the sequential tunneling transitions to and from the N electron excited state gives rise to an increase in the current. By measuring the differential conductance a spectroscopy of excited states can be performed.² *Within* the Coulomb diamond the N electron ground state is stable with respect to sequential tunneling. If the tunnel coupling to the leads is weak, the transport is suppressed within the Coulomb diamond. As the tunnel coupling is enhanced transport becomes possible as a result of higher order tunneling processes. At low bias voltage, $V < \Delta$, only *elastic co-tunneling* is allowed by energy conservation. Charge is transported through the dot without exciting it. At higher bias voltage, $V \geq \Delta$, *inelastic co-tunneling* processes excite the dot and give rise to an additional current. Since these processes transfer energy between the dot and the leads, the co-tunneling is called inelastic.⁹ The dot switches between the N electron ground and excited state and in certain cases the $N \pm 1$ electron ground states can be occupied, too. These two regimes are considered separately in the next two sections. We point out that the model introduced here can be applied to a limited range of bias and gate voltages in an experimental situation where the capacitances and single particle energies provide a sufficiently accurate parametrization of the many-body spectrum of the dot.

III. ELASTIC CO-TUNNELING

At low bias voltage $V < \Delta$, a tunneling process of second order in the transition amplitude cannot populate the excited state. However, in this order of tunneling, transport is possible via elastic co-tunneling without exciting the dot. This is the dominant contribution to the current at sufficiently low temperatures and voltages. We do not consider here the integer-spin Kondo physics on a small energy scale T_K , which has recently been observed:^{5,6} we assume $T, V \gg T_K$. It was pointed out in Refs.^{10,11} that elastic co-tunneling is the only process limiting the operation of a quantum dot as a single electron transistor when the level quantization δ is comparable with the charging energy U .

In a co-tunneling process two tunneling events occur in a very short time interval. For instance, an electron is first injected into the dot from the left lead and then emitted to the right lead. On this small time scale the two tunneling events are coherent. The energy of the total system (dot and leads) is sufficiently uncertain for the process not to be completely blocked. However, the transition amplitude for this process is inversely proportional to the energy difference between the initial and intermediate state of the total system.¹² The amplitude for transferring an electron in the opposite sequence (first emit an electron, then inject one) via another intermediate state must also be added if the final state of the system is the same. From the total second order amplitude (or matrix element) one obtains the tunneling rate by statistically averaging over all initial and final states of the leads.⁹ Thus a current can pass through the dot although the $N - 1$ and $N + 1$ electron states are only virtually accessible.

Let us describe the calculation of the tunneling rate for this simple case in order to skip the details of similar calculations below. Consider the initial state of the system where two electrons are in level l of the left leads and the dot in the ground state, denoted by $|N_{0,0}\rangle a_{l\uparrow}^\dagger a_{l\downarrow}^\dagger |\rangle$ where $|\rangle$ denotes the state of the other electrons in the noninteracting leads. Applying the tunneling operators H_{TLD}^\dagger and H_{RLd} in the two possible sequences, one obtains the final state $|N_{0,0}\rangle \hat{F} |\rangle$ where the operator \hat{F} is given in Table I. The amplitude for this process is written as $\sqrt{2}M_{N \leftarrow N}$ where the factor $\sqrt{2}$ is due to the spin degeneracy of the levels in the left lead. The explicit expression for $M_{N \leftarrow N}$ is given in Table II. Introducing the tunneling rate

$$\Gamma_{N \leftarrow N} = 2\pi \sum_{l,r} |M_{N \leftarrow N}|^2 f(\varepsilon_l - \mu_L) [1 - f(\varepsilon_r - \mu_R)] \delta(\varepsilon_l - \varepsilon_r), \quad (10)$$

we write for the elastic co-tunneling current

$$I = 2\Gamma_{N \leftarrow N}. \quad (11)$$

The sum over all possible states of the leads with the Fermi distribution $f(\varepsilon) = 1/(1 + e^{\varepsilon/T})$ can be converted into an integration and gives

$$\begin{aligned} \Gamma_{N \leftarrow N} = \frac{1}{2\pi} & \left[\Gamma_{dd}^L \Gamma_{dd}^R \tau(E_{NN-1}, V) + \Gamma_{d'd'}^L \Gamma_{d'd'}^R \tau(E_{N+1N}, V) \right. \\ & \left. + \Gamma_{dd'}^L \Gamma_{d'd}^R \tau'(E_{NN-1}, E_{N+1N}, V) \right] \end{aligned} \quad (12)$$

Here we introduced the rates $\Gamma_{dd}^L = 2\pi \sum_l |t_{ld}|^2 \delta(\varepsilon - \varepsilon_l)$ and $\Gamma_{d'd'}^L$ ($d \rightarrow d'$) for sequential tunneling into level d and d' and we assumed that these depend only weakly on the energy ε . The same applies to the quantity $\Gamma_{dd'}^L = 2\pi \sum_l t_{ld}^* t_{ld'} \delta(\varepsilon - \varepsilon_l)$ in the last term on the right-hand side of Eq. (12), which takes into account the interference between the two possible sequences for the tunneling events (“paths” in energy space); $\Gamma_{dd'}^R, \Gamma_{dd}^R, \Gamma_{d'd'}^R$ are defined similarly ($L, l \rightarrow R, r$). All these quantities are treated as parameters here. In the expression for the rate (12) the explicit (V) and implicit dependence [through the addition energies; cf. Eqs. (6)] on the voltages is incorporated in the functions (explicitly evaluated in the limit $T \rightarrow 0$)

$$\tau(E, V) = \int_{-\infty}^{\infty} d\varepsilon \frac{f(\varepsilon - \mu_L) [1 - f(\varepsilon - \mu_R)]}{(\varepsilon - E)^2} \quad (13a)$$

$$\begin{aligned} &= \frac{V}{(\mu_L - E)(\mu_R - E)} \Theta(V), \\ \tau'(E, E', V) &= \int_{-\infty}^{\infty} d\varepsilon \frac{f(\varepsilon - \mu_L) [1 - f(\varepsilon - \mu_R)]}{|\varepsilon - E| |\varepsilon - E'|} \\ &= \frac{1}{|E' - E|} \left(\left| \ln \frac{\mu_L - E}{\mu_R - E} \right| + \left| \ln \frac{\mu_L - E'}{\mu_R - E'} \right| \right) \Theta(V), \end{aligned} \quad (13b)$$

Here Θ is the unit step function and $\lim_{E' \rightarrow E} \tau'(E, E', V) = \tau(E, V)$. The voltage dependence will be important below. The rate (12) diverges near the edges of the Coulomb diamond where sequential tunneling becomes dominant [cf. condition (3)]. Here the second order perturbation theory for the amplitudes breaks down. However, well within the Coulomb diamond we have $\Gamma_{N \leftarrow N} \ll \Gamma_{dd'}^{L,R}, \Gamma_{dd}^{L,R}, \Gamma_{d'd'}^{L,R}$ and perturbation theory can be used. This is the regime of interest here.

IV. INELASTIC CO-TUNNELING

If the bias voltage can supply the necessary excitation energy, $V \geq \Delta$, then the excited state can be populated by inelastic co-tunneling events.⁹ In such a coherent process, an electron is transferred from the left to the right lead, thereby loosing an amount Δ of its excess energy, which is supplied by the transport voltage; this energy is transferred to the dot, which is thereby excited. The excited state can relax to the N electron ground state by two sorts of processes depending on Δ . If Δ is sufficiently small then there is an energy barrier for injecting or emitting electrons [i.e. conditions (7a) and (7b) are not satisfied]. Thus the excited state is also Coulomb blockaded. The dot can relax by three different inelastic co-tunneling processes. An electron can be transferred from the left to the right lead again, but now gain an energy Δ , thereby relaxing the dot. Similarly, an electron injected from either lead can be excited above the Fermi level of that same lead. The dot relaxes without a net charge transfer. This is the situation in the region labeled (I) in Fig. 1. For the current the elastic co-tunneling through the excited state is also important. If Δ is sufficiently large, however, the excited state can decay to the ground state by two sequential tunneling processes. There are three possibilities. Either the dot can relax to the $N-1$ electron ground state and then return to the N electron ground state [region (II) in Fig. 1]; or the dot can be excited to the $N+1$ electron ground state from which it returns to the N electron ground state [region (II')]; or both processes can occur [region (III)]. For positive bias voltage these regions are delimited by the bias voltage threshold lines [Eqs. (4) and (9)] as follows:

$$\begin{aligned} (I) \quad \Delta & < V < V_L^{N'N-1}, V_L^{N+1N'} \quad \Delta < \frac{1}{3} V_{\max}^N \\ (II) \quad \Delta, V_R^{N'N-1} & < V < V_R^{NN-1}, V_L^{N+1N'} \quad \Delta < \frac{1}{2} V_{\max}^N \\ (II') \quad \Delta, V_L^{N+1N'} & < V < V_L^{N+1N}, V_L^{N'N-1} \quad \Delta < \frac{1}{2} V_{\max}^N \\ (III) \quad \Delta, V_R^{N'N-1}, V_L^{N+1N'} & < V < V_R^{NN-1}, V_L^{N+1N} \quad \Delta < V_{\max}^N \end{aligned}$$

Depending on the excitation energy $\Delta = \delta - J$ relative to the maximum bias voltage $V_{\max}^N = \delta + U$ some of these regions do not exist. The different limiting cases are depicted in Fig. 2. When the excitation energy is sufficiently small, $\Delta < V_{\max}^N/3$, all these regions exist. From this we find that the Coulomb and/or exchange interaction should be large relative to the level spacing: $\delta < \frac{1}{2}U + \frac{3}{2}J$. Region (I) ceases to exist for larger values of Δ (or δ) while regions (II) and (II') continue to exist as long as $\Delta < V_{\max}^N/2$, i.e., $\delta < U + 2J$. Region (III) always exists since $\Delta < V_{\max}^N$ is satisfied for $U + J > 0$. The situation is clearly more complicated than at low voltage $V < \Delta$. The transport in each region needs to be considered separately. Below we first consider the simplest region (I), where only the ground and excited state participate in the transport. Then we extend this analysis to the other regions.

A. Region I - relaxation by co-tunneling

This region exists only when the excited state lies sufficiently close to the ground state. There are four states involved in the transport, of which three are degenerate. In order to calculate the current we need the nonequilibrium occupation of the states in the dot. We assume that at the bias voltage where inelastic co-tunneling processes become important, $V \sim \Delta$, the lifetime of the states in the dots is much smaller than the typical time scale for building up Kondo-type correlations between the leads and dots system. In terms of energies we thus assume $T_K \ll \Delta < V \ll \Gamma$ where T_K is the energy scale for such correlations. In this limit we can use the following master equations¹³ to describe the occupation of the ground state $\rho_{N_{0,0}}$ and of the three triplet excited states $\rho_{N'_{1,m}}, m = 0, \pm 1$:

$$\partial_t \rho_{N_{0,0}} = \sum_{i=1,2,3} \Gamma_{N \leftarrow N'}^{(i)} \sum_{m=0,\pm 1} \rho_{N'_{1,m}} - 3\Gamma_{N' \leftarrow N} \rho_{N_{0,0}}, \quad (14a)$$

$$\partial_t \rho_{N'_{1,0}} = \Gamma_{N' \leftarrow N} \rho_{N_{0,0}} + \frac{1}{2} \Gamma_{N' \leftarrow N'}^{(1)} \sum_{m=\pm 1} \rho_{N'_{1,m}} - \left[\Gamma_{N' \leftarrow N'}^{(1)} + \sum_{i=1,2,3} \Gamma_{N \leftarrow N'}^{(i)} \right] \rho_{N'_{1,0}}, \quad (14b)$$

$$\partial_t \rho_{N'_{1,m}} = \Gamma_{N' \leftarrow N} \rho_{N_{0,0}} + \frac{1}{2} \Gamma_{N' \leftarrow N'}^{(1)} \rho_{N'_{1,0}} - \left[\frac{1}{2} \Gamma_{N' \leftarrow N'}^{(1)} + \sum_{i=1,2,3} \Gamma_{N \leftarrow N'}^{(i)} \right] \rho_{N'_{1,m}}, \quad (14c)$$

where $m = \pm 1$ and $\rho_{N_{0,0}} + \sum_{m=0,\pm 1} \rho_{N'_{1,m}} = 1$. The current reads

$$I = (2\Gamma_{N \leftarrow N} + 3\Gamma_{N' \leftarrow N}) \rho_{N_{0,0}} + \left(\frac{1}{2} \Gamma_{N' \leftarrow N'}^{(1)} + \Gamma_{N' \leftarrow N'}^{(2)} + \Gamma_{N \leftarrow N'}^{(1)} \right) \sum_{m=0,\pm 1} \rho_{N'_{1,m}}. \quad (15)$$

The transitions between the states are schematically indicated in Fig. 3. The rates are calculated using the Golden Rule as was done for Eq. (12). In Table I we have listed the final state of the leads, the matrix element and the transition rate for each transition. The explicit expressions for the matrix elements are given in Table II. Let us now calculate these rates and discuss the transitions that they describe starting with the inelastic co-tunneling processes.

Each excited state of the triplet is populated by inelastic co-tunneling transition from the ground state with the same rate $\Gamma_{N' \leftarrow N}$. An electron with energy ε_l and spin $s = \pm 1/2$ is first injected into the dot from lead L , bringing the dot in the intermediate state $|N+1\rangle_{1/2,s}$, and is subsequently emitted into the lead R at an energy $\varepsilon_r = \varepsilon_l - \Delta$. The other sequence is also possible, in which case the intermediate state of the dot is $|N-1\rangle_{1/2,-s}$. The sum of the amplitudes for these processes yields the matrix element $M_{N' \leftarrow N}$, listed in Table II. The inelastic co-tunneling rate for exciting the dot is then reads [cf. Eqs. (13a) and (13b)]

$$\Gamma_{N' \leftarrow N} = 2\pi \sum_{l,r} |M_{N' \leftarrow N}|^2 f(\varepsilon_l - \mu_L) [1 - f(\varepsilon_r - \mu_R)] \delta(\varepsilon_l - \varepsilon_r - \Delta) \quad (16a)$$

$$= \frac{1}{2\pi} \Gamma_{d'd}^L \Gamma_{dd}^R [\tau(E_{NN-1}, V - \Delta) + \tau(E_{N+1N} - \Delta, V - \Delta) + 2\tau'(E_{NN-1}, E_{N+1N} - \Delta, V - \Delta)] \quad (16b)$$

Conversely, each state of the triplet can relax to the singlet ground state by inelastic co-tunneling. The rate for these processes must be calculated separately because they result in a different final state of the leads. The matrix

element $M_{N \leftarrow N'}^{(1)}$ in Table II describes the transfer of an electron from the left to the right lead starting in any of the three triplet sublevels of the excited state. The energy of the emitted electron is increased by the excitation energy $\varepsilon_r = \varepsilon_l + \Delta$. The inelastic co-tunneling rate for this relaxation process is [cf. Eq. (8)]

$$\Gamma_{N \leftarrow N'}^{(1)} = 2\pi \sum_{l,r} \left| M_{N \leftarrow N'}^{(1)} \right|^2 f(\varepsilon_l - \mu_L) [1 - f(\varepsilon_r - \mu_R)] \delta(\varepsilon_l + \Delta - \varepsilon_r) \quad (17a)$$

$$= \frac{1}{2\pi} \Gamma_{d'd}^L \Gamma_{dd}^R [\tau(E_{N'N-1}, V + \Delta) + \tau(E_{N+1N'} + \Delta, V + \Delta) + 2\tau'(E_{N'N-1}, E_{N+1N'} + \Delta, V + \Delta)]. \quad (17b)$$

This rate explicitly depends on the voltage because the voltage window (both μ_L and μ_R appear in the Fermi functions). The second process involves the injection of an electron at energy ε_l from the left lead and the emission of an electron to an empty state in the same lead at a higher energy $\varepsilon_{l'} = \varepsilon_l + \Delta$. The matrix element $M_{N \leftarrow N'}^{(2)}$ is thus found by replacing $r \rightarrow l'$, cf. Table II. The tunneling rate is similarly found by replacing $r, R \rightarrow l', L$ in Eq. (17a) and from the result (17b) we obtain:

$$\Gamma_{N \leftarrow N'}^{(2)} = \frac{\Gamma_{dd}^L}{\Gamma_{dd}^R} \Gamma_{N \leftarrow N'}^{(1)} (V = 0).$$

The third process involves the injection and emission of an electron to and from the right lead: replacing $L \rightarrow R$ we find:

$$\Gamma_{N \leftarrow N'}^{(3)} = \frac{\Gamma_{d'd'}^R}{\Gamma_{d'd'}^L} \Gamma_{N \leftarrow N'}^{(1)} (V = 0).$$

Let us now consider the elastic co-tunneling processes in which electrons are transferred from the left to the right lead. These involve four spin-degenerate intermediate states of the dot. In addition to the four ground states (1), there are four other intermediate *excited* states

$$\begin{aligned} |(N-1)'_{1/2,+1/2}\rangle &= a_{d'\uparrow}^\dagger |0\rangle, & |(N+1)'_{1/2,+1/2}\rangle &= a_{d'\uparrow}^\dagger a_{d'\downarrow}^\dagger a_{d\uparrow}^\dagger |0\rangle, \\ |(N-1)'_{1/2,-1/2}\rangle &= a_{d'\downarrow}^\dagger |0\rangle, & |(N+1)'_{1/2,-1/2}\rangle &= a_{d'\uparrow}^\dagger a_{d'\downarrow}^\dagger a_{d\downarrow}^\dagger |0\rangle. \end{aligned}$$

The addition energies for the transitions from the N electron excited state to these states are

$$\begin{aligned} E_{N'N-1'} &= E_{NN-1} + \Delta - \delta = E_{NN-1} + J, \\ E_{N+1'N'} &= E_{N+1N} + \delta - \Delta = E_{N+1N} - J. \end{aligned}$$

These energies lie closer to the Fermi energies than E_{NN-1} and E_{N+1N} . Therefore the contributions of these intermediate states to elastic co-tunneling amplitudes are larger than those in the amplitude $M_{N \leftarrow N}$ and they cannot be disregarded. Three types of elastic co-tunneling processes must be considered separately. Two of these processes do not involve a flip of the spin of the transmitted electron. The two different final states of the leads as indicated in Table I. The first type of process occurs with the same rate $\frac{1}{2} \Gamma_{N' \leftarrow N'}^{(1)}$ for all states of the triplet. The second type is only possible for the two states with nonzero spin projection and occurs with a rate $\frac{1}{2} \Gamma_{N' \leftarrow N'}^{(2)}$. The rates are calculated from the matrix elements $M_{N' \leftarrow N'}^{(1,2)}$ in Table II and give [compare this with Eq. (12)]

$$\Gamma_{N' \leftarrow N'}^{(1,2)} = 2\pi \sum_{l,r} \left| M_{N' \leftarrow N'}^{(1,2)} \right|^2 f(\varepsilon_l - \mu_L) [1 - f(\varepsilon_r - \mu_R)] \delta(\varepsilon_l - \varepsilon_r) \quad (20a)$$

$$\begin{aligned} &= \frac{1}{2\pi} \{ \Gamma_{dd}^L \Gamma_{dd}^R [\tau(E_{N'N-1}, V) + \tau(E_{N+1N'}, V) \pm 2\tau'(E_{N'N-1}, E_{N+1N'}, V)] \\ &\quad + \Gamma_{d'd'}^L \Gamma_{d'd'}^R [\tau(E_{N'N-1'}, V) + \tau(E_{N+1'N'}, V) \pm 2\tau'(E_{N'N-1'}, E_{N+1'N'}, V)] \\ &\quad + 2 \operatorname{Re} \Gamma_{dd'}^L \Gamma_{d'd}^R [\tau'(E_{N'N-1}, E_{N'N-1'}, V) \pm \tau'(E_{N'N-1}, E_{N+1'N'}, V) \\ &\quad \pm \tau'(E_{N+1N'}, E_{N+1'N'}, V) \pm \tau'(E_{N'N-1'}, E_{N+1N'}, V)] \}. \end{aligned} \quad (20b)$$

These processes do not induce transitions between the states [they do not contribute to Eqs. (14)], but they do contribute to the transfer of electrons [the rate appears in Eq. (15)]. The third type of elastic co-tunneling process,

involves a flip of the spin of the transmitted electron and induces transitions between the triplet states states. The triplet state $|N'_{1,0}\rangle$ can decay to both $|N'_{1,1}\rangle$ and $|N'_{1,-1}\rangle$ with a rate equal to $\frac{1}{2}\Gamma_{N' \leftarrow N'}^{(2)}$. The latter two states can return to the former state with the same transition rate.

Because there is no Zeeman energy or spin-orbit coupling in our model, the transition rates between the states of the triplet balance each other, cf. Fig. 3. Therefore we can introduce the total occupations of the excited state $\rho_{N'} \equiv \sum_{m=0,\pm 1} \rho_{N'_{1,m}}$ summed over the spin projection and omit the spin indices $\rho_N \equiv \rho_{N_{0,0}}$. By adding the equations for the triplet states we obtain a closed set of master equations for the total occupations:

$$\partial_t \rho_N = \sum_{i=1,2,3} \Gamma_{N \leftarrow N'}^{(i)} \rho_{N'} - 3\Gamma_{N' \leftarrow N} \rho_N, \quad (21a)$$

$$\partial_t \rho_{N'} = 3\Gamma_{N' \leftarrow N} \rho_N - \sum_{i=1,2,3} \Gamma_{N \leftarrow N'}^{(i)} \rho_{N'}, \quad (21b)$$

with $\rho_N + \rho_{N'} = 1$. The elastic co-tunneling transitions between the triplet states have precisely cancelled. However, these processes do contribute to the current (15). The fact that the triplet state with zero spin projection transfers twice as much charge per unit time ($2 \times \frac{1}{2}\Gamma_{N' \leftarrow N'}^{(2)}$) as the other states ($\frac{1}{2}\Gamma_{N' \leftarrow N'}^{(2)}$) is precisely balanced by the spin-flip processes that can only occur for states with nonzero spin projection ($\frac{1}{2}\Gamma_{N' \leftarrow N'}^{(2)}$). The elastic co-tunneling contribution of each state of the triplet is thus proportional to the same rate (15) and we can also express the current in total occupations

$$I = (2\Gamma_{N \leftarrow N} + 3\Gamma_{N' \leftarrow N}) \rho_N + \left(\frac{1}{2}\Gamma_{N' \leftarrow N'}^{(1)} + \Gamma_{N' \leftarrow N'}^{(2)} + \Gamma_{N \leftarrow N'}^{(1)} \right) \rho_{N'}. \quad (22)$$

Note that the inelastic co-tunneling relaxation processes with rates $\Gamma_{N \leftarrow N'}^{(2,3)}$ do not appear here since they do not involve charge transfer. In the stationary limit $\lim_{t \rightarrow \infty} \partial_t \rho_{N'}, \partial_t \rho_N = 0$ equations (21) are readily solved. The current can be written as

$$I = \frac{\left(\frac{1}{2}\Gamma_{N' \leftarrow N'}^{(1)} + \Gamma_{N' \leftarrow N'}^{(2)} - 2\Gamma_{N \leftarrow N} \right) + 2\Gamma_{N \leftarrow N'}^{(1)} + \sum_{i=2,3} \Gamma_{N \leftarrow N'}^{(i)}}{\sum_{i=1,2,3} \Gamma_{N \leftarrow N'}^{(i)} + 3\Gamma_{N' \leftarrow N}} 3\Gamma_{N' \leftarrow N} + 2\Gamma_{N \leftarrow N}. \quad (23)$$

For $V < \Delta$ the excitation rate $\Gamma_{N' \leftarrow N}$ vanishes and we recover the elastic co-tunneling current 11. In Fig. 4 we have plotted the current, differential conductance and the co-tunneling rates as a function of bias voltages for the case $\Delta < V_{\max}^N/3$. In this limit region (I) covers most of the Coulomb diamond for $V \geq \Delta$. Apart from a clear kink in the current and a step in the differential conductance, a sharp peak is present at the step edge. This is clearly due to a change of the population of the excited state.

B. Regions (II), (II') and (III) - relaxation by sequential tunneling

The remain three regions where sequential tunneling transitions from the excited state to $N - 1$ and/or $N + 1$ electron ground state are possible are now easily included. The elastic co-tunneling processes involving the excited state must now be disregarded (and their contributions to the current). The rates for these processes diverge at the boundaries of regime (I) signalling that perturbation theory breaks down. Instead we write a full set of master equations similar to (14) without the transitions between the triplet states and now including the occupations of the spin sublevels of the $N - 1$ and/or $N + 1$ electron ground states. Proceeding as before we arrive at the following closed set of master equations for the total occupations, including $\rho_{N \pm 1} \equiv \sum_{m=\pm 1/2} \rho_{(N \pm 1)_{1/2,m}}$:

$$\partial_t \rho_{N-1} = \alpha_- \Gamma_{d'd'}^R \rho_{N'} - (\alpha_- \Gamma_{dd}^R + \alpha_+ \Gamma_{d'd'}^L) \rho_{N-1}, \quad (24a)$$

$$\partial_t \rho_{N+1} = \alpha_+ \Gamma_{dd}^L \rho_{N'} - (\alpha_- \Gamma_{d'd'}^L + \alpha_+ \Gamma_{d'd'}^R) \rho_{N+1}, \quad (24b)$$

$$\partial_t \rho_N = +\alpha_- \Gamma_{dd}^L \rho_{N-1} + \alpha_+ \Gamma_{d'd'}^R \rho_{N+1} - 3\Gamma_{N' \leftarrow N} \rho_N, \quad (24c)$$

$$\begin{aligned} \partial_t \rho_{N'} = & \alpha_- \Gamma_{d'd'}^L \rho_{N-1} + \alpha_+ \Gamma_{dd}^R \rho_{N+1} + 3\Gamma_{N' \leftarrow N} \rho_N \\ & - (+\alpha_- \Gamma_{d'd'}^R \rho_{N'} + \alpha_+ \Gamma_{dd}^L \rho_{N'}) \rho_{N'}, \end{aligned} \quad (24d)$$

The current reads

$$I = (2\Gamma_{N \leftarrow N} + 3\Gamma_{N' \leftarrow N}) \rho_N + \alpha_- \Gamma_{d'd'}^R \rho_{N'} + \alpha_+ (\Gamma_{dd}^R + \Gamma_{d'd'}^R) \rho_{N+1}. \quad (25)$$

These expression covers regions (II) [$\alpha_- = 1, \alpha_+ = 0$], (II') [$\alpha_- = 0, \alpha_+ = 1$] and (III) [$\alpha_\pm = 1$]. The solution for all cases can be written in the form

$$I = \frac{2K + K' - 2\kappa\Gamma_{N \leftarrow N} + 2\Gamma_{N' \leftarrow N}^{(1)}}{K + 3\kappa\Gamma_{N' \leftarrow N}} 3\Gamma_{N' \leftarrow N} + 2\Gamma_{N \leftarrow N}. \quad (26)$$

The coefficients appearing here are constants that characterize the differences between the three regions:

$$\begin{aligned} K &= \alpha_- \Gamma_{d'd'}^R \frac{\Gamma_{dd}^L}{\Gamma_{dd}^L + \Gamma_{d'd'}^L} + \alpha_+ \Gamma_{d'd'}^L \frac{\Gamma_{dd}^R}{\Gamma_{dd}^R + \Gamma_{d'd'}^R}, \\ K' &= \alpha_- \Gamma_{d'd'}^R \frac{\Gamma_{d'd'}^L}{\Gamma_{dd}^L + \Gamma_{d'd'}^L} + \alpha_+ \Gamma_{d'd'}^L \frac{\Gamma_{d'd'}^R}{\Gamma_{dd}^R + \Gamma_{d'd'}^R}, \\ \kappa &= \alpha_- \frac{\Gamma_{d'd'}^R}{\Gamma_{dd}^L + \Gamma_{d'd'}^L} + \alpha_+ \frac{\Gamma_{d'd'}^L}{\Gamma_{dd}^R + \Gamma_{d'd'}^R} + 1. \end{aligned}$$

where $K + K' = \alpha_- \Gamma_{d'd'}^R + \alpha_+ \Gamma_{d'd'}^L$. In Fig. 5 we have plotted the co-tunneling rates, the occupations of the states and the differential conductance as a function of the bias voltages for $\Gamma_{dd}^\alpha = \Gamma_{d'd'}^\alpha = \Gamma, \alpha = L, R$ for a typical case where $V_{\max}^N/2 \leq \Delta$. In this limit only region (III) exists. The qualitative result is the same as in region (I). The essential condition for the peak in the conductance is that the total rate for charge transport through the excited state is bigger than the rate $\Gamma_{N' \leftarrow N}$ at which this state is populated.

V. CONCLUSIONS

We have analyzed the finite bias transport *within* a Coulomb blockaded region of a quantum dot with an even number of electrons. The differential conductance through the dot was found to exhibit a step within the Coulomb diamond at a bias voltage equal to the excitation energy. At the step edge an additional peak appears that is caused by a change in the nonequilibrium populations of the dot states due the voltage dependence of the co-tunneling rates. This may explain the recent observations in the transport spectroscopy of semi-conductor quantum dots by De Franceschi et. al and of carbon nanotubes by Nygård et. al. As pointed out in Ref.³ the sharp feature in the differential conductance can be used to do a spectroscopy of excited states with increased resolution. We have considered two well-separated regimes where the excited state is depopulated by inelastic co-tunneling and sequential tunneling, respectively. It is expected that in the crossover regime the results do not change qualitatively since the inelastic co-tunneling processes that excite the dot form the bottleneck for the transport. The rate for these processes as calculated here is correct also in the crossover regime. The calculations presented here can be improved by including (additive) contributions of more virtual states of the dot (more than two orbitals) to the transition amplitudes, which determine the co-tunneling rates. Also, the situation where a second N -electron excited state lies the Coulomb diamond can be treated in the same way as single excited state. The occupations of all transport states can be calculated from an extended set of master equations. One must now also include co-tunneling transitions between the two excited states. The rates that enter in these equations have the same form as those calculated here. Furthermore, the peak at the onset of inelastic co-tunneling is broadened by thermal fluctuations and level broadening effects, as pointed out in Ref.³. The effect of a electron finite temperature can be included in our calculations. Level broadening effects require a nonperturbative scheme, which is beyond the scope of this chapter. It is clear, however, that near the onset of inelastic co-tunneling, the broadening of the peak, which is determined the decay rate of the excited state (either by sequential or inelastic co-tunneling), is much larger than the rate for exciting the dot.

VI. ACKNOWLEDGEMENTS

We would like to thank S. De Franceschi for bringing this problem to our attention and for useful discussions. One of us (M.R.W) would like to thank M. Eto and Y. Tokura for valuable discussions. This work is part of the research program of the “Stichting voor Fundamenteel Onderzoek der Materie” (FOM), which is financially supported by the “Nederlandse Organisatie voor Wetenschappelijk Onderzoek” (NWO) and the NEDO project NTDP-98.

¹ L. P. Kouwenhoven, C. M. Marcus, P. L. McEuen, S. Tarucha, R. M. Westervelt, and N. S. Wingreen, in *Proceedings of the NATO Advanced Study Institute on Mesoscopic Electron Transport*, Eds. L. L. Sohn, L. P. Kouwenhoven, and G. Schön (Kluwer Series E345, 1997).

² L. P. Kouwenhoven, T. H. Oosterkamp, M. W. S. Danoesastro, M. Eto, D. G. Austing, T. Honda, and S. Tarucha, *Science* **278**, 1788 (1997).

³ S. De Franceschi, S. Sasaki, J. M. Elzerman, W. G. van der Wiel, S. Tarucha, L. P. Kouwenhoven, *Phys. Rev. Lett.* **86**, 878 (2001).

⁴ J. Nygård, D. H. Cobden, P. E. Lindelof, *Nature* **408**, 342 (2000).

⁵ S. Sasaki, S. De Franceschi, J. M. Elzerman, W. G. van der Wiel, M. Eto, S. Tarucha, and L. P. Kouwenhoven, *Nature* **405**, 764-767 (2000).

⁶ M. Pustilnik, L. I. Glazman, D. H. Cobden, and L.P. Kouwenhoven, cond-mat/0010336 (unpublished).

⁷ M. Pustilnik, Y. Avishai, and K. Kikoin, *Phys. Rev. Lett.* **84** (2000).

⁸ M. Eto, *Jpn. J. Appl. Phys.* **40** Part 1, No 3B (2001).

⁹ D. V. Averin and Yu. V. Nazarov, *Phys. Rev. Lett.* **65**, 2446 (1990);
D. V. Averin and Yu. V. Nazarov, in *Single Charge Tunneling - Coulomb Blockade Phenomena in Nanostructures*, Eds. H. Grabert and M.H. Devoret (Plenum Press and NATO Scientific Affairs Division, New York, 1992).

¹⁰ D.C. Glattli, *Physica B* **189**, 88 (1993).

¹¹ K. Kang, B. I. Min, *Phys. Rev. B* **55**, 15412 (1997).

¹² R. P. Feynman and A. R. Hibbs, *Quantum Mechanics and Path Integrals* (McGraw-Hill, New York, 1965), Chapter 6.

¹³ D. V. Averin, A. N. Korotkov, and K. K. Likharev, *Phys. Rev. B* **44**, 6199 (1991);
C. W. J. Beenakker, *Phys. Rev. B* **44**, 1646 (1991);
Y. Meir, N. S. Wingreen, and P. A. Lee, *Phys. Rev. Lett.* **66**, 3048 (1991).

TABLE I. Transitions from initial state $|i\rangle a_{l\uparrow}^{\dagger} a_{l\downarrow}^{\dagger} |$ to final state $|f\rangle \hat{F} |$ with the second order matrix elements and corresponding rates. The explicit expressions for the matrix elements are given in Table II. The rates are given in the text. Here l and r' label occupied states in the left and right lead, respectively; l' and r label unoccupied states in the left and right lead, respectively.

type	$i \rightarrow$	f	\hat{F}	$ M_{Ff \leftarrow iI} $	$\Gamma_{f \leftarrow i}$
elastic	$N_{0,0}$	$N_{0,0}$	$\frac{1}{\sqrt{2}} (a_{l\downarrow}^{\dagger} a_{r\uparrow}^{\dagger} - a_{l\uparrow}^{\dagger} a_{r\downarrow}^{\dagger})$	$\sqrt{2} M_{N \leftarrow N}$	$2\Gamma_{N \leftarrow N}$
inelastic	$N_{0,0}$	$N'_{1,0}$	$\frac{1}{\sqrt{2}} (a_{l\downarrow}^{\dagger} a_{r'\uparrow}^{\dagger} + a_{l'\uparrow}^{\dagger} a_{r\downarrow}^{\dagger})$	$M_{N' \leftarrow N}$	$\Gamma_{N' \leftarrow N}$
	$N_{0,0}$	$N'_{1,+1}$	$a_{l\downarrow}^{\dagger} a_{r\downarrow}^{\dagger}$		
	$N_{0,0}$	$N'_{1,-1}$	$a_{l\downarrow}^{\dagger} a_{r\uparrow}^{\dagger}$		
elastic	$N'_{1,m}$	$N'_{1,m}, m = \pm 1, 0$	$\frac{1}{\sqrt{2}} (a_{l\downarrow}^{\dagger} a_{r'\uparrow}^{\dagger} - a_{l'\uparrow}^{\dagger} a_{r\downarrow}^{\dagger})$	$M_{N' \leftarrow N'}^{(1)}/\sqrt{2}$	$\frac{1}{2}\Gamma_{N' \leftarrow N'}^{(1)}$
	$N'_{1,m}$	$N'_{1,m}, m = \pm 1 (!)$	$\frac{1}{\sqrt{2}} (a_{l\downarrow}^{\dagger} a_{r'\uparrow}^{\dagger} + a_{l'\uparrow}^{\dagger} a_{r\downarrow}^{\dagger})$	$M_{N' \leftarrow N'}^{(2)}/\sqrt{2}$	$\frac{1}{2}\Gamma_{N' \leftarrow N'}^{(2)}$
	$N'_{1,0}$	$N'_{1,+1}$	$a_{l\downarrow}^{\dagger} a_{r\downarrow}^{\dagger}$	$M_{N' \leftarrow N'}^{(2)}/\sqrt{2}$	$\frac{1}{2}\Gamma_{N' \leftarrow N'}^{(2)}$
	$N'_{1,0}$	$N'_{1,-1}$	$a_{l\downarrow}^{\dagger} a_{r\uparrow}^{\dagger}$		
	$N'_{1,+1}$	$N'_{1,0}$	$a_{l\downarrow}^{\dagger} a_{r\uparrow}^{\dagger}$		
	$N'_{1,-1}$	$N'_{1,0}$	$a_{l\downarrow}^{\dagger} a_{r\downarrow}^{\dagger}$		
inelastic	$N'_{1,0}$	$N_{0,0}$	$\frac{1}{\sqrt{2}} (a_{l\downarrow}^{\dagger} a_{r'\uparrow}^{\dagger} + a_{l'\uparrow}^{\dagger} a_{r\downarrow}^{\dagger})$	$M_{N \leftarrow N'}^{(1)}$	$\Gamma_{N \leftarrow N'}^{(1)}$
	$N'_{1,+1}$	$N_{0,0}$	$a_{l\downarrow}^{\dagger} a_{r\uparrow}^{\dagger}$		
	$N'_{1,-1}$	$N_{0,0}$	$a_{l\downarrow}^{\dagger} a_{r\downarrow}^{\dagger}$		
	$N'_{1,0}$	$N_{0,0}$	$\frac{1}{\sqrt{2}} (a_{l\downarrow}^{\dagger} a_{l'\uparrow}^{\dagger} + a_{l'\uparrow}^{\dagger} a_{l\downarrow}^{\dagger})$	$M_{N \leftarrow N'}^{(2)}$	$\Gamma_{N \leftarrow N'}^{(2)}$
	$N'_{1,+1}$	$N_{0,0}$	$a_{l\downarrow}^{\dagger} a_{l'\uparrow}^{\dagger}$		
	$N'_{1,-1}$	$N_{0,0}$	$a_{l\downarrow}^{\dagger} a_{l'\downarrow}^{\dagger}$		
	$N'_{1,0}$	$N_{0,0}$	$\frac{1}{\sqrt{2}} (a_{r'\downarrow}^{\dagger} a_{r\uparrow}^{\dagger} + a_{r'\uparrow}^{\dagger} a_{r\downarrow}^{\dagger})$	$M_{N \leftarrow N'}^{(3)}$	$\Gamma_{N \leftarrow N'}^{(3)}$
	$N'_{1,+1}$	$N_{0,0}$	$a_{r'\downarrow}^{\dagger} a_{r\uparrow}^{\dagger}$		
	$N'_{1,-1}$	$N_{0,0}$	$a_{r'\downarrow}^{\dagger} a_{r\downarrow}^{\dagger}$		

TABLE II. Second order matrix elements for the transitions listed in Table I.

$M_{N \leftarrow N}$	$=$	$\frac{t_{ld}^* t_{rd}}{\varepsilon_r - E_{NN-1}} + \frac{t_{ld'}^* t_{rd'}}{E_{N+1N} - \varepsilon_l}$	elastic
$M_{N' \leftarrow N'}^{(1,2)}$	$=$	$\frac{t_{ld}^* t_{rd}}{\varepsilon_r - E_{N'N-1}} + \frac{t_{ld'}^* t_{rd'}}{\varepsilon_r - E_{N'N-1'}} \\ \pm \left(\frac{t_{ld}^* t_{rd}}{E_{N+1N'} - \varepsilon_l} + \frac{t_{ld'}^* t_{rd'}}{E_{N+1N'} - \varepsilon_l} \right)$	
$M_{N' \leftarrow N}$	$=$	$\frac{t_{ld'}^* t_{rd}}{\varepsilon_r - E_{NN-1}} + \frac{t_{ld'}^* t_{rd}}{E_{N+1N} - \varepsilon_l}$	inelastic
$M_{N \leftarrow N'}^{(1)}$	$=$	$\frac{t_{ld}^* t_{rd'}}{\varepsilon_r - E_{N'N-1}} + \frac{t_{ld}^* t_{rd'}}{E_{N+1N'} - \varepsilon_l}$	
$M_{N \leftarrow N'}^{(2)}$	$=$	$\frac{t_{ld}^* t_{ld'}}{\varepsilon_r - E_{N'N-1}} + \frac{t_{ld}^* t_{ld'}}{E_{N+1N'} - \varepsilon_l}$	
$M_{N \leftarrow N'}^{(3)}$	$=$	$\frac{t_{r'd}^* t_{rd'}}{\varepsilon_r - E_{N'N-1}} + \frac{t_{r'd}^* t_{rd'}}{E_{N+1N'} - \varepsilon_r}$	

FIG. 1. Stability diagram of a quantum dot for the symmetric case $C_L/C_G = C_R/C_G \gg 1$. The skewed lines delimit the regions where sequential tunneling is possible through the ground states [thick; Eqs. (4)] and the excited state [thin; Eqs. (9)]. The horizontal thick lines mark the onset of inelastic co-tunneling.

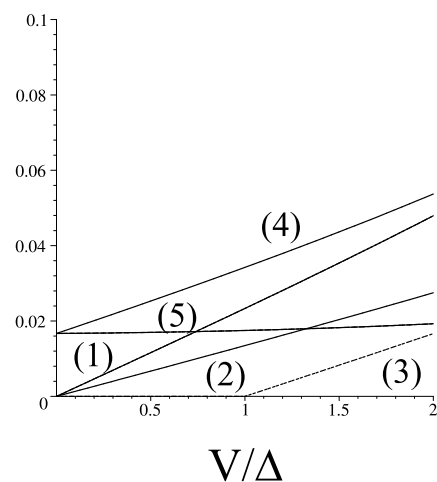
FIG. 2. Inelastic co-tunneling regions for the different cases of excitation energy relative to the maximal bias voltage.

FIG. 3. Transitions between the spin-singlet ground state and the spin-triplet excited state. Elastic co-tunneling processes which do not change the state (charge and spin projection) are indicated by a circle, beginning and ending at the same state.

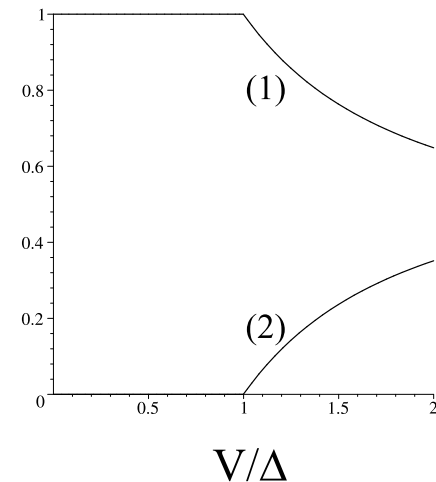
FIG. 4. Results for region (I) as a function of bias voltage in the center of the Coulomb diamond: $\Delta/V_{\max}^N = 0.1$, $\delta/U = 5$, $U = 1$, $\Gamma/U = 0.05$, $C_L/C_G = C_R/C_G = 0.1$. *Left:* Co-tunneling rates relative to the sequential tunneling rate, i.e., in units of Γ . Elastic: (1) for the N electron ground state $\Gamma_{N \leftarrow N}$ (2) for the N electron excited state $\Gamma_{N' \leftarrow N'}^{(1)} = \Gamma_{N' \leftarrow N'}^{(2)}$. Inelastic: (3) for exciting the dot $\Gamma_{N' \leftarrow N}$ (4) for relaxing the dot with charge transfer $\Gamma_{N \leftarrow N'}^{(1)}$ and (5) without charge transfer $\Gamma_{N \leftarrow N'}^{(2,3)}$. *Middle:* Occupations of (1) the N electron ground state (2) the N electron excited state and (3) the $N-1$ and $N+1$ electron ground states (coincide). *Right:* Differential conductance calculated from expression (23) for the current.

FIG. 5. Results in region (III) as a function of bias voltage in the center of the Coulomb diamond: $\Delta/V_{\max}^N = 0.5$, $\delta/U = 5$, $U = 1$, $\Gamma/U = 0.04$, $C_L/C_G = C_R/C_G = 0.1$. *Left:* Co-tunneling rates relative to the sequential tunneling rate, i.e., in units of Γ . Elastic: (1) for the N electron ground state $\Gamma_{N \leftarrow N}$. Inelastic: (2) for exciting the dot $\Gamma_{N' \leftarrow N}$. *Middle:* Occupations of (1) the N electron ground state (2) the N electron excited state and (3) the $N-1$ and $N+1$ electron ground states (coincide). *Right:* Differential conductance calculated from expression (26) for the current.

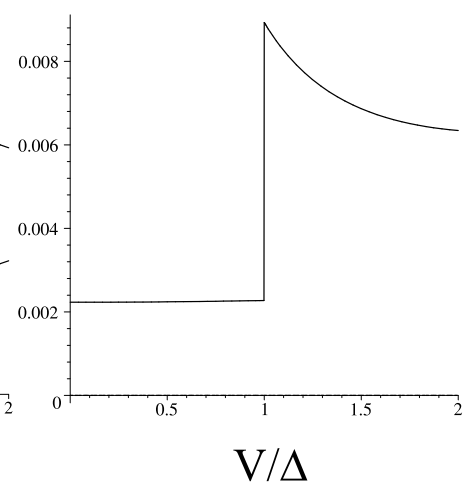
Co-tunneling rates



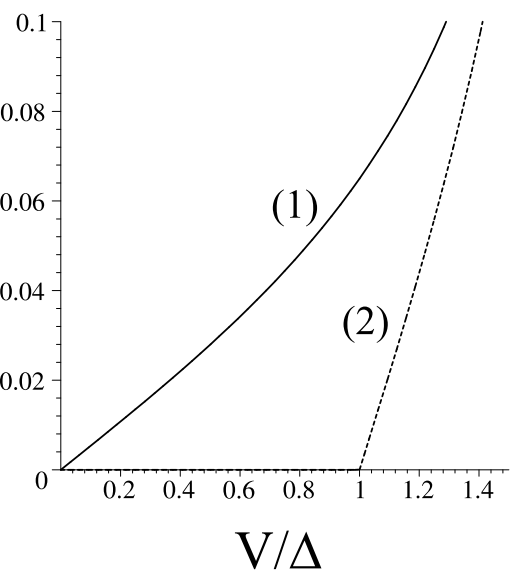
Occupations



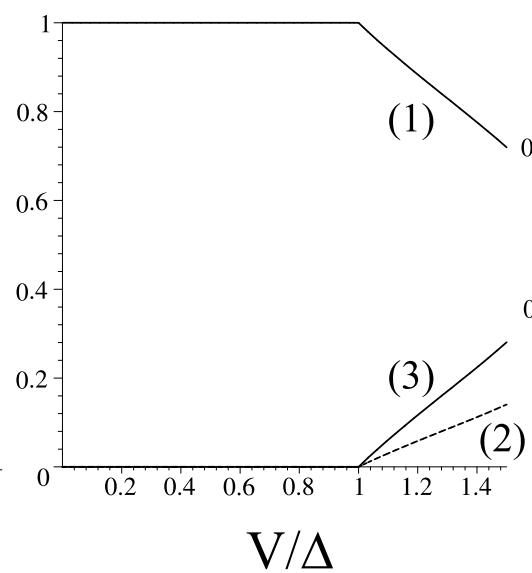
Differential conductance



Co-tunneling rates



Occupations



Differential conductance

